Co-Optimization of Communication and Motion Planning of a Robotic Operation in Fading Environments

Yuan Yan and Yasamin Mostofi
ECE Department, University of New Mexico, Albuquerque, NM 87113, USA
{yuanyan, ymostofi}@ece.unm.edu

***Abstract*— In this paper, we consider the scenario where a robot needs to maximize the amount of information it sends to a fixed station as it moves along a predefined trajectory. We consider the case where the robot operates under energy and time constraints and has to jointly consider its motion and communication costs. We then show how the robot can co-optimize its velocity, motion energy and transmission rate/power along the trajectory, by using our recently-proposed probabilistic wireless channel assessment framework. Our mathematical analysis and simulation results show how our proposed co-optimization framework results in a considerably more efficient use of the available resources.**

I. Introduction

In recent years, considerable progress has been made in the area of networked robotic systems. Issues related to the navigation and control of such systems have been heavily explored in the robotics/control community [1], [2]. Similarly, there is a rich literature on the communication and networking aspects of mobile ad hoc networks, in the communication and signal processing communities [3]–[5]. In order to truly realize the full potential of these systems, however, an integrative approach to both communication and navigation issues is needed.

In recent years, such communication-aware navigation approaches have started to attract considerable attention. In [6], the authors show how a robot can optimize its trajectory by considering both communication link qualities and sensing/navigation issues. In [7], Fiedler eigenvalue is adopted as a connectivity metric to improve the communication qualities in a robotic network. In [8], the authors use a spring-mass model to guarantee the connectivity, assuming that disk models can represent the channels. In [9], the authors design a stop-go strategy to increase the average transmission rate of a robot in fading environments. In [10], the authors use mixed-integer programming to solve a robotic router problem. In [11], the authors propose an efficient algorithm to find the path that minimizes the total energy cost, assuming simplified path loss models to represent the channels. In [12], it is shown how to design robotic networks in realistic communication environments.

In several scenarios, a robot has to operate under resource constraints such as energy and/or time. Then, the robot needs to decide how to spend its available resources along its trajectory, by considering both its communication and navigation costs, in realistic fading environments. This is the main motivation of the work presented here. In this paper, we aim to design both the communication and motion strategies of a networked robotic operation, under energy and time constraints, in realistic fading environments. More specifically, we consider a scenario where a robot needs to transmit as many bits of information as possible to a fixed station, under both energy and time constraints, as it moves along a predefined trajectory. The predefined trajectory could be due to the existence of several obstacles in the workspace, which can limit the navigation of the robot to a constrained route. The contribution of this paper is then as follows. We show how the robot can plan its navigation speed, communication transmission rate, as well as transmission power over the trajectory, given the limited energy and time resources. This co-optimization, in realistic fading environments, requires an assessment of the link qualities at places over the predefined trajectory that have not yet been visited by the robot. We show how our previously-proposed probabilistic channel prediction framework of [13], [14] allows the robot to assess the shadowing and path loss components of the channel over the trajectory and plan for using its limited energy and time resources. Furthermore, we show how the robot can further fine tune its resource allocation, by using an additional water-filling approach, as it moves along its trajectory and measures the true value of the channel. We also prove a number of properties about our proposed framework. To the best of our knowledge, co-optimization of communication and navigation strategies over a given trajectory, in fading environments, under time and energy constraints has not been previously explored.

The rest of the paper is organized as follows. Section II describes the communication and motion models and briefly discusses the probabilistic channel assessment framework of [13], [14]. Section III presents our proposed optimization framework, based on the probabilistic assessment of shadowing and path loss terms, and proves a number of properties of the optimum solution. Section IV then shows how the robot can furthermore fine tune its resource allocation as it travels along its trajectory, based on its online channel measurements. The section also shows the conditions under which this additional fine tuning can be beneficial. Finally, section V shows the performance of the proposed framework in a simulation environment. This is followed by conclusions in Section VI.

This work is supported by NSF CAREER award # 0846483.

II. Problem Setup

Consider the scenario where a robot needs to maximize the amount of information it sends to a fixed station, as it moves along a predefined trajectory $\mathcal{T}$ with length L. The predefined trajectory could be the only feasible path, for instance, due to environmental constraints such as obstacles. Fig. 1 shows an example of the considered scenario. The robot starts from an initial position, follows the direction of $\mathcal{T}$, and transmits as many bits of information as possible to a fixed base station before reaching its terminal position. We assume limited energy and time budgets for the operation. In order to optimize the performance, the robot is then required to properly allocate its available resources based on the quality of the channel to the base station along its trajectory. To do so, however, the robot needs to have an assessment of the channel to the base station along $\mathcal{T}$. In this section, we present our system model and introduce our previously-proposed probabilistic channel assessment framework [13], [14] that enables the robot to assess the channel quality at unvisited locations along its trajectory, based on a small number of channel measurements.

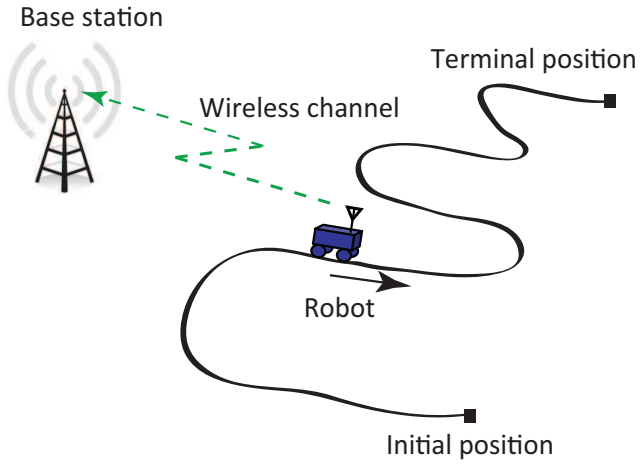

Fig. 1. The robot needs to send as many bits as possible to the base station while traveling along a predefined trajectory, under time and energy constraints.

A. Probabilistic Modeling of a Wireless Channel

A fundamental parameter that characterizes the performance of a communication channel is the received Channel to Noise Ratio (CNR), defined as the ratio of the received channel power to the receiver thermal noise power. As shown in the communication literature [15], received CNR can be modeled as a multi-scale random process with three dynamics: path loss, shadow fading (shadowing) and multipath fading. Let $\gamma(q)$ denote the received CNR in the transmission from a robot at position q to the base station. By using a 2D non-stationary random field model, we have the following characterization for $\gamma(q)$ (in dB): $\gamma_{\text{dB}}(q) = \alpha_{\text{dB}} - 10\,n\log_{10}\big(\|q-q_b\|\big) + \gamma_{\text{SH}}(q) + \gamma_{\text{MP}}(q)$, where $\gamma_{\text{dB}}(q) = 10\log_{10}\big(\gamma(q)\big)$, q_b is the position of the base station, and $\gamma_{\text{SH}}(q)$ and $\gamma_{\text{MP}}(q)$ are independent random variables, representing the effects of shadowing and multipath fading in dB respectively [15]. The distance-dependent path loss has a linear decay in the dB domain. Then, α_{dB} and $-10\,n$ represent its offset and slope respectively.

1) Probabilistic Wireless Channel Assessment Based on a Small Number of Channel Measurements [13], [14]: In this part, we briefly summarize how the robot can probabilistically assess the spatial variations of the instantaneous received CNR of the base station along its trajectory, using a small number of CNR measurements available at the beginning of the operation.

Let $\mathcal{Q} = \{q_1, \cdots, q_m\}$, for $m = |\mathcal{Q}|$, denote the set of the positions corresponding to the small number of CNR measurements available to the robot. The stacked vector of the available received CNR measurements (in dB) can then be expressed by $Y = H_q\theta + \omega + v$, where $H_q = [\mathbf{1}_m \quad -D_q]$, $\mathbf{1}_m$ denotes the m-dimensional vector of all ones, $D_q = \big[10\log_{10}(\|q_1-q_b\|) \;\cdots\; 10\log_{10}(\|q_m-q_b\|)\big]^{\text{T}}$, $\theta = [\alpha_{\text{dB}} \quad n]^{\text{T}}$, $\omega = \big[\gamma_{\text{SH}}(q_1) \;\cdots\; \gamma_{\text{SH}}(q_m)\big]^{\text{T}}$ and $v = \big[\gamma_{\text{MP}}(q_1) \;\cdots\; \gamma_{\text{MP}}(q_m)\big]^{\text{T}}$. Based on the commonly-used lognormal distribution for shadow fading and its reported exponential spatial correlation [15], ω is a zero-mean Gaussian random vector with the covariance matrix $\Omega \in \mathbb{R}^{m\times m}$, where $\big[\Omega\big]_{i,j} = \xi^2_{\text{dB}}\exp(-\|q_i-q_j\|/\beta)$ for $i,j \in \{1,\cdots,m\}$, with ξ^2_{dB} and β denoting the variance of the shadow fading component in dB and its *decorrelation distance* respectively. Let ρ^2_{dB} represent the power of multipath fading component (in dB) and I_m be the m-dimensional identity matrix. We have the following lemma for estimating the underlying model parameters:

Lemma 1: Define $\chi \triangleq \xi^2_{\text{dB}} + \rho^2_{\text{dB}}$. Then, the Least Square (LS) estimation of the channel parameters are given as follows:

$$\hat{\theta} = (H_q^{\text{T}}H_q)^{-1}H_q^{\text{T}}Y, \qquad \hat{\chi} = \frac{1}{m}Y_{H_q}^{\text{T}}Y_{H_q},$$
$$\hat{\xi}^2_{\text{dB}}, \hat{\beta} = \min_{\xi^2_{\text{dB}},\beta} \sum_{d\in\mathcal{L}(d)} \tau(d)\left(\xi^2_{\text{dB}}\exp(-d/\beta) - \hat{r}(d)\right)^2,$$
$$\hat{\rho}^2_{\text{dB}} = \hat{\chi} - \hat{\xi}^2_{\text{dB}},$$

where $Y_{H_q} = \big(I_m - H_q(H_q^{\text{T}}H_q)^{-1}H_q^{\text{T}}\big)Y$ represents the centered version of the measurement vector, $\hat{r}(d) = \big(\sum_{(i,j)\in\mathcal{S}(d)}\big[Y_{H_q}\big]_i\big[Y_{H_q}\big]_j\big)/|\mathcal{S}(d)|$ is the numerical estimate of the spatial correlation at distance d, with $\mathcal{S}(d) = \big\{(i,j) \;\big|\; q_i,q_j \in \mathcal{Q}, \big\|q_i-q_j\big\| = d\big\}$. Furthermore, $\tau(d)$ is a weight that can be chosen based on the assessment of the accuracy of the estimation of $\hat{r}(d)$ and $\mathcal{L}(d) = \big\{d \mid 0 < \hat{r}(d) < \hat{\chi}\big\}$.

Proof: See [13], [14] for the proof. ∎

Then, based on the measurements available to the robot and conditioned on the channel parameters, the assessment of the received CNR at a set of points $x = [x_1^{\text{T}} \;\cdots\; x_N^{\text{T}}]^{\text{T}}$, along the trajectory of the robot is given by the following lemma:

Lemma 2: Assume a set of points $x = [x_1^{\text{T}} \;\cdots\; x_N^{\text{T}}]^{\text{T}}$ along $\mathcal{T}$, such that $x_i \notin \mathcal{Q}$. Then, a Gaussian distribution with the following mean $\Upsilon_{\text{dB}}(x) = \mathbb{E}\big\{\gamma_{\text{dB}}(x) \;\big|\; Y,\theta,\beta,\xi_{\text{dB}},\rho_{\text{dB}}\big\}$ and covariance $\Sigma(x) = \mathbb{E}\Big\{\big(\gamma_{\text{dB}}(x)-\Upsilon_{\text{dB}}(x)\big)\big(\gamma_{\text{dB}}(x)-\Upsilon_{\text{dB}}(x)\big)^{\text{T}} \,\Big|\, Y,\theta,\beta,\xi_{\text{dB}},\rho_{\text{dB}}\Big\}$

can best characterize the shadowing and path loss components of CNR at x:

$$\Upsilon_{\text{dB}}(x) = H_x\,\theta + \Psi^{\text{T}}(x)\Phi^{-1}\big(Y - H_q\theta\big), \tag{1}$$

$$\Sigma(x) = \Pi(x) + \rho^2_{\text{dB}} I_N - \Psi^{\text{T}}(x)\Phi^{-1}\Psi(x), \tag{2}$$

where $H_x = [\mathbf{1}_N \;\; -D_x]$, $D_x = \big[10\log_{10}(\|x_1 - q_b\|)\cdots 10\log_{10}(\|x_N - q_b\|)\big]^{\text{T}}$, $\Phi = \Omega + \rho^2_{\text{dB}} I_m$, $\big[\Pi(x)\big]_{i,j} = \xi^2_{\text{dB}}\exp(-\|x_i - x_j\|/\beta)$ and $\big[\Psi(x)\big]_{i,j} = \xi^2_{\text{dB}}\exp(-\|q_i - q_j\|/\beta)$.

Proof: See [13], [14] for the proof. ■

B. Spectral Efficiency and Communication Cost

In this paper, we assume M-QAM modulation for the transceivers of the robot and the base station. Let $p_b(\gamma) = \text{Prob}\{b \neq \hat{b}\}$ denote the bit error rate, where b and $\hat{b}$ represent a transmitted bit (as part of a transmitted packet) and its reception (after passing through a decision device) respectively. Then, we have the following approximated expression [15]: $p_b(\gamma) \approx 0.2\exp\left(-1.5\,P\gamma/(M-1)\right)$, where M represents the modulation constellation size and P denotes the communication transmit power. This approximation is tight (within 1 dB) when $0 < 10\log_{10}(P\gamma) < 30$ dB [15]. The spectral efficiency is then characterized as follows [15]: $R = \log_2(M) = \log_2(1 + KP\gamma)$, where $K = -1.5/\ln(5p_{b,\text{th}})$, and $p_{b,\text{th}}$ is the maximum tolerable bit error rate for robust operation.

C. Motion Cost

In this paper, we assume that the robot uses a DC motor for its motion. Based on the permanent magnet DC motor model, the motion power can be characterized as follows [16]:

$$P_{\text{M}} = \kappa_1 u^2 + \kappa_2 u + \kappa_3, \tag{3}$$

where P_{M} is the motion power, u denotes the velocity of the robot, and κ_1, κ_2 and κ_3 are positive constants depending on the parameters of the motor, external load and the transmission system of the robot. Eq. 3 neglects the impact of acceleration since it is negligible for many DC motors [17]. Consider the case where it takes t seconds for the robot to travel over a fixed length l. We have the following motion energy:

$$E_{\text{M}} = \underbrace{\frac{\kappa_1 l^2}{t} + \kappa_3 t}_{\widetilde{E}_{\text{M}}} + \kappa_2 l. \tag{4}$$

Since we assume a fixed trajectory, the control input, u, only affects $\widetilde{E}_{\text{M}}$. Hence, we use $\widetilde{E}_{\text{M}}$ instead of E_{M} to denote the motion energy cost when formulating our optimization framework in Section III.

III. Co-Optimization of Motion and Communication Costs

In this section, we show how the robot can co-optimize both its communication and motion to maximize the number of information bits transmitted to the base station, given its limited time and energy resources.

We divide the whole trajectory into N equal-length sub-trajectories, $\mathcal{T}_i$, for $i \in \{1, 2, \cdots, N\}$, each with length of $l = L/N$. We assume small enough l such that the path loss and shadowing components of the channel can be assumed constant along each $\mathcal{T}_i$. Note that the channel is still space-varying over each $\mathcal{T}_i$ due to multipath fading. In this section, we show how the robot can optimize its communication and motion, based on its prediction of the shadowing and path loss components of the channel over the sub-trajectories. More specifically, we show how the robot can decide 1) how much time to spend and 2) how much energy to allocate for its motion and communication along each sub-trajectory. In Section IV, we then show how the robot can furthermore fine tune its strategies by adapting to multipath fading as it moves along each sub-trajectory and measures the true value of the channel.

Assume that the robot starts with a number of initial CNR measurements collected a priori in the same environment where it is operating. It can then use the aforementioned probabilistic channel assessment framework of Section II-A to predict the path loss and shadowing components of the received CNR over each sub-trajectory $\mathcal{T}_i$. Let $x = [x_1^{\text{T}} \cdots x_N^{\text{T}}]^{\text{T}}$ for $x_i \in \mathcal{T}_i$ represent a set of points along the trajectory of the robot. Then the path loss and shadowing components of the channel can be estimated by evaluating Eq. 1. By using the motion and communication models of the previous section, the following optimization problem maximizes the total number of transmitted bits per Hertz, under the time and energy constraints of the system (note that the given bandwidth is fixed):

$$\begin{aligned}
\text{maximize} \quad & \mathcal{J} = \sum_{i=1}^{N} \log_2(1 + P_i K \Upsilon_i) t_i \\
\text{subject to} \quad & \sum_{i=1}^{N} \underbrace{P_i t_i}_{E_{\text{C},i}=\text{comm. cost}} + \underbrace{\frac{\kappa_1 l^2}{t_i} + \kappa_3 t_i}_{\widetilde{E}_{\text{M},i}=\text{motion cost}} \leq E, \\
& \sum_{i=1}^{N} t_i \leq T,\; P_i,\; t_i \geq 0,\; \forall\; i \in \{1, \cdots, N\},
\end{aligned} \tag{5}$$

where P_i and t_i denote the optimum communication transmission power and time allocated to the i^{th} sub-trajectory respectively and E and T are the total energy and time budgets for the whole operation respectively. In this formulation, we assume that the robot travels at a constant speed along each sub-trajectory. Also, we take E to be finite and lower bounded by $E_{\min}$, where $E_{\min} = \begin{cases} \kappa_1 L^2/T + \kappa_3 T & \text{if } T < \sqrt{\kappa_1/\kappa_3}L \\ 2\sqrt{\kappa_1\kappa_3}L & \text{otherwise} \end{cases}$. This ensures that E is larger than the minimum required motion energy to reach the terminal position. Then, the maximum number of bits that the robot can send is always larger than 0.

There is no closed-form solution for Eq. 5. However, we are still able to characterize certain properties of the optimum solution as we show next. In what follows, we use superscript $*$ to represent the optimal solution (or value) of the corresponding optimization problem.

Definition 1 (LICQ, [18]): The Linear Independence Constraint Qualification (LICQ) holds if the gradients of the active constraints are linearly independent.

Theorem 1: Suppose that x^* is a local solution of an optimization problem, that the objective function and the constraints are continuously differentiable, and that the LICQ holds at x^*, then there exists a Lagrange multiplier vector λ^* such that Karush-Kuhn-Tucker (KKT) conditions hold at (x^*, λ^*).

Proof: See [18]. ■

Due to the boundedness of E, we have $t_i > 0$ for all i, i.e. constraints $t_i \geq 0$ are always inactive. The gradients of the power and time constraints (in case of being active) with respect to the vector of variables $\left[P_1 \cdots P_N | t_1 \cdots t_N\right]^{\mathrm{T}}$ are given as $\left[t_1 \cdots t_N | P_1 - \kappa_1 l^2/t_1^2 + \kappa_3 \cdots P_N - \kappa_1 l^2/t_N^2 + \kappa_3\right]^{\mathrm{T}}$, $\left[\mathbf{0}_N^{\mathrm{T}} \mid \mathbf{1}_N^{\mathrm{T}}\right]^{\mathrm{T}}$ and $\left[e_i^{\mathrm{T}} \mid \mathbf{0}_N^{\mathrm{T}}\right]^{\mathrm{T}}$ (for any i where $P_i = 0$), where $\mathbf{0}_N$ denotes the N-dimensional vector of all zeros, and e_i represents the N-dimensional unit vector with the i^{th} entry equal to 1. Therefore, the gradients of the active constraints are linearly independent if there exists an i such that $P_i > 0$. Clearly, $P_i = 0$ for all i is not a solution if E is larger than the minimum required motion energy. Therefore, the KKT conditions hold for Eq. 5.

Lemma 3: The optimal solution of Eq. 5 satisfies the following properties: if $\Upsilon_i > \Upsilon_j$, then $P_i^* \geq P_j^*$ and $t_i^* \geq t_j^*$.

Proof: We have the following for the dual function of the optimization problem of Eq. 5: $f_{\mathcal{J}} = -\sum_{i=1}^{N} \log_2(1 + P_i K \Upsilon_i) t_i - \sum_{i=1}^{N} \mu_i P_i - \sum_{i=1}^{N} \epsilon_i t_i + \lambda \left(\sum_{i=1}^{N} P_i t_i + \kappa_1 l^2/t_i + \kappa_3 t_i - E \right) + \nu \left(\sum_{i=1}^{N} t_i - T \right)$, where μ_i, ϵ_i, ν and λ are Lagrange multipliers. The optimum solution of Eq. 5 should satisfy the following Karush-Kuhn-Tucker (KKT) conditions:

$$\frac{\partial f_{\mathcal{J}}}{\partial P_i} = -\frac{1}{\ln 2} \frac{K \Upsilon_i}{1 + P_i K \Upsilon_i} t_i + \lambda t_i - \mu_i = 0, \tag{6}$$

$$\frac{\partial f_{\mathcal{J}}}{\partial t_i} = -\log_2(1 + P_i K \Upsilon_i) + \nu - \epsilon_i + \lambda \left(P_i - \frac{\kappa_1 l^2}{t_i^2} + \kappa_3 \right) = 0, \tag{7}$$

$\lambda \left(\sum_{i=1}^{N} P_i t_i + \kappa_1 l^2/t_i + \kappa_3 t_i - E \right) = 0$, $\epsilon_i t_i = 0$, $\nu \left(\sum_{i=1}^{N} t_i - T \right) = 0$, $\mu_i P_i = 0$, and $t_i, P_i, \mu_i, \epsilon_i, \lambda, \nu \geq 0$. Since the total given energy is bounded, we have $t_i > 0$ for all i, resulting in $\epsilon_i = 0$ for all i . Moreover, Eq. 6 and 7 can further be simplified as follows:

$$P_i^* = \begin{cases} \frac{1}{\lambda^* \ln 2} - \frac{1}{K \Upsilon_i} & \text{if } i \in \mathcal{I}, \\ 0 & \text{otherwise}, \end{cases} \tag{8}$$

$$\frac{\kappa_1 l^2}{t_i^{*2}} = \begin{cases} -\frac{1}{\lambda^*} \log_2 \left(\frac{K \Upsilon_i}{\lambda^* \ln 2} \right) + \frac{1}{\lambda^* \ln 2} \\ \quad -\frac{1}{K \Upsilon_i} + \frac{\nu^*}{\lambda^*} + \kappa_3 & \text{if } i \in \mathcal{I}, \\ \frac{\nu^*}{\lambda^*} + \kappa_3 & \text{otherwise}, \end{cases} \tag{9}$$

where $\mathcal{I} = \{i \in \{1, \cdots, N\} \mid \Upsilon_i > \lambda^* \ln 2/K\}$. It can be seen that $P_i^* = 0$ if Υ_i is below the threshold $\lambda^* \ln 2/K$. Furthermore, for $i \in \mathcal{I}$, P_i^* increases as Υ_i increases. Hence $P_i^* > P_j^*$ if $\Upsilon_i > \Upsilon_j$, for $i \in \mathcal{I}$ and any j. Furthermore, $P_i^* = P_j^* = 0$ for $i, j \in \{1, \cdots, N\} \setminus \mathcal{I}$. Similarly, $t_i^* > t_j^*$ if $\Upsilon_i > \Upsilon_j$, for $i \in \mathcal{I}$ and any j. Moreover, $t_i^* = t_j^*$ if $i, j \in \{1, \cdots, N\} \setminus \mathcal{I}$. ■

Lemma 3 shows that the robot will allocate more transmit power and time to the places that have a better communication quality. If the communication quality is too low, the robot will not allocate any transmit power.

Corollary 1: The optimal solution of Eq. 5 satisfies the following property: if $\Upsilon_i > \Upsilon_j$, then $P_{\mathrm{M},i}^* \leq P_{\mathrm{M},j}^*$.

Proof: Note that $P_{\mathrm{M},i} = \kappa_1 u_i^2 + \kappa_2 u_i + \kappa_3$ is a monotonically increasing function of u_i for $u_i > 0$. From Lemma 3, we have $t_i^* \geq t_j^*$ if $\Upsilon_i > \Upsilon_j$. Hence, $P_{\mathrm{M},i}^* \leq P_{\mathrm{M},j}^*$ if $\Upsilon_i > \Upsilon_j$. ■

Corollary 1 shows that the robot will allocate more motion power to the places that have a worse communication quality, in order to escape from these regions faster.

IV. Online Fine Tuning and Adaptation to Multipath fading

As mentioned previously, the channel in each $\mathcal{T}_i$ is space-varying due to multipath fading, especially in rich scattering environments. Unlike path loss and shadowing, the multipath fading component of the channel is unpredictable. A common optimal approach to mitigate the multipath fading is the water-filling technique [15], assuming that the statistical knowledge of the multipath fading component is available. In this section, we show how the robot can implement a water-filling strategy as it moves along its trajectory and measures the real value of the channel. We furthermore analyze the asymptotic performance of the water-filling strategy in the case of high average CNR.

Assume that the distribution of the multipath fading component in $\mathcal{T}_i$ is learned (for instance by using Lemma 1). Let P_i^* be the optimal average transmit power budget assigned to $\mathcal{T}_i$, using the optimization problem of Eq. 5. Then, we have the following water-filling optimization problem over $\mathcal{T}_i$ [15]:

$$\begin{aligned} \text{maximize} \quad & \int_0^{\infty} \log_2(1 + K \widetilde{P}_i(\gamma_i) \gamma_i) p(\gamma_i) d\gamma_i, \\ \text{subject to} \quad & \int_0^{\infty} \widetilde{P}_i(\gamma_i) p(\gamma_i) d\gamma_i = P_i^*, \end{aligned} \tag{10}$$

where $\widetilde{P}_i(\gamma_i)$ represents the instantaneous transmit power as a function of γ_i and $p(\gamma_i)$ denotes the pdf of the multipath fading of the i^{th} sub-trajectory. The solution of Eq. 10 can be found as follows:

$$\widetilde{P}_i(\gamma_i) = \begin{cases} \frac{1}{\sigma_i^* \ln 2} - \frac{1}{K \gamma_i} & \text{if } \gamma_i \geq \frac{\sigma_i^* \ln 2}{K}, \\ 0 & \text{otherwise}, \end{cases} \tag{11}$$

where σ_i^* satisfies the following condition: $\int_{\sigma_i^* \ln 2/K}^{\infty} \left(1/(\sigma_i^* \ln 2) - 1/(K \gamma_i)\right) p(\gamma_i) d\gamma_i = P_i^*$. As can be seen in Eq. 11, the water-filling approach

allows the robot to adapt the transmit power online in order to combat the multipath fading, based on the instantaneous CNR. Then the optimal performance can be found by substituting Eq. 11 into the objective function: $\int_{\sigma_i^* \ln 2/K}^{\infty} \log_2 \left(K\gamma_i/(\sigma_i^* \ln 2)\right) p(\gamma_i) d\gamma_i$.

Next, we show the asymptotic property of the water-filling approach as $\overline{\gamma}_i = \mathbb{E}\{\gamma_i\} \to \infty$. Assume that the pdf of the multipath fading component satisfies the following two properties for any $a > 0$: 1) $\int_a^{\infty} p(\gamma_i) d\gamma_i \to 1$ as $\overline{\gamma}_i \to \infty$; 2) $\int_a^{\infty} p(\gamma_i)/\gamma_i d\gamma_i \to 0$ as $\overline{\gamma}_i \to \infty$. Note that the assumptions above are not limiting since most of the commonly-used multipath fading models, such as Nakagami, lognormal, and Rayleigh, satisfy them. For example, for the case of Nakagami fading with parameter $m_i \geq 0.5$ in $\mathcal{T}_i$, the first assumption is satisfied since

$$\int_a^{\infty} \left(\frac{m_i}{\overline{\gamma}_i}\right)^{m_i} \frac{\gamma_i^{m_i-1}}{\Gamma(m_i)} \exp\left(-\frac{m_i\gamma_i}{\overline{\gamma}_i}\right) d\gamma_i$$
$$= \int_{am_i/\overline{\gamma}_i}^{\infty} \frac{z_i^{m_i-1}}{\Gamma(m_i)} \exp\left(-z_i\right) dz_i = \frac{\Gamma_{\mathrm{I}}(m_i, am_i/\overline{\gamma}_i)}{\Gamma(m_i)} \to 1$$

as $\overline{\gamma}_i \to \infty$, where $\Gamma(\cdot)$ and $\Gamma_{\mathrm{I}}(\cdot)$ denote the gamma function and upper incomplete gamma function respectively. The second assumption can be verified as follows:

$$\int_a^{\infty} \frac{1}{\gamma_i} \left(\frac{m_i}{\overline{\gamma}_i}\right)^{m_i} \frac{\gamma_i^{m_i-1}}{\Gamma(m_i)} \exp\left(-\frac{m_i\gamma_i}{\overline{\gamma}_i}\right) d\gamma_i$$
$$= \frac{m_i}{\overline{\gamma}_i} \int_{am_i/\overline{\gamma}_i}^{\infty} \frac{z_i^{m_i-2}}{\Gamma(m_i)} \exp\left(-z_i\right) dz_i. \quad (12)$$

Clearly, $\int_{am_i/\overline{\gamma}_i}^{\infty} z_i^{m_i-2} \exp\left(-z_i\right) dz_i \leq \Gamma(m_i - 1)$ and is finite if $m_i > 1$. Then, Eq. 12 approaches 0 as $\overline{\gamma}_i \to \infty$. For the case of $0.5 \leq m_i \leq 1$, the limit of Eq. 12 can be found as follows: $1/(a\Gamma(m_i)) \left(am_i/\overline{\gamma}_i\right)^{m_i} \exp\left(-am_i/\overline{\gamma}_i\right) \to 0$. Hence, Nakagami fading model also satisfies the second assumption.

Based on the two assumptions above, we then have the following asymptotic property of the water-filling approach.

Lemma 4: If the pdf of the multipath fading component satisfies the assumptions above, then the benefit of additional water-filling is negligible as $\overline{\gamma}_i \to \infty$.

Proof: As $\overline{\gamma}_i \to \infty$, we have $\sigma_i^* = 1/(P_i^* \ln 2)$ since $\int_{1/(P_i^* K)}^{\infty} \left(P_i^* - 1/(K\gamma_i)\right) p(\gamma_i) d\gamma_i = P_i^*$. Then the performance gap between additional water-filling approach and constant power allocation becomes the following:

$$0 \leq \int_{\sigma_i^* \ln 2/K}^{\infty} \log_2 \left(\frac{K\gamma_i}{\sigma_i^* \ln 2}\right) p(\gamma_i) d\gamma_i$$
$$- \int_0^{\infty} \log_2(1 + KP_i^*\gamma_i) p(\gamma_i) d\gamma_i$$
$$\leq \int_{\sigma_i^* \ln 2/K}^{\infty} \log_2 \left(\frac{K\gamma_i}{\sigma_i^* \ln 2}\right) p(\gamma_i) d\gamma_i$$
$$- \int_{\sigma_i^* \ln 2/K}^{\infty} \log_2(KP_i^*\gamma_i) p(\gamma_i) d\gamma_i$$
$$= \int_{\sigma_i^* \ln 2/K}^{\infty} \log_2 \left(\frac{1}{\sigma_i^* P_i^* \ln 2}\right) p(\gamma_i) d\gamma_i. \quad (13)$$

By substituting $\sigma_i^* = 1/(P_i^* \ln 2)$ into Eq. 13, the performance gap becomes 0. Hence we conclude that the benefit of additional water-filling is negligible, as $\overline{\gamma}_i \to \infty$. ■

Consider the case that the channel is well estimated along the trajectory. From Lemma 3, we then expect that the overall performance is dominated by the $\mathcal{T}_i$s that have high CNR since the available resources are mainly allocated to these regions. The analysis above says that the benefits of the additional water-filling become smaller if average CNR is high. Hence, if $\overline{\gamma}_i$s are large enough at least in some $\mathcal{T}_i$s (i.e. the channel quality is not low along the whole trajectory), the additional water-filling does not result in a noticeable performance improvement. Thus, in this case, our co-optimization framework can achieve a good performance without any knowledge of the multipath fading and adaptation to it.

However, if the channel quality is low everywhere along the trajectory, then the additional water-filling can further provide a non-negligible performance improvement.

V. Simulation Results

Consider the case where the base station is at $(0, 0)$, the predefined trajectory is a line from $(0, 100)$ to $(200, 100)$, and $N = 80$. The channel is generated by our probabilistic channel simulator [19] with the following parameters: $n = 4$, $\beta = 10$m, $\xi_{\mathrm{dB}} = 8$, resolution $= 0.1$m. The multipath fading is taken to be uncorrelated Rayleigh fading. Therefore, there are 2000 discrete points to represent the entire channel and the channel is assumed to be constant in each 0.1m interval. As can be seen in Fig. 2 (top), the channel is dominated by the shadowing and multipath fading.

We take $T = 1000$, $E = 1300$ and $\kappa_1 = \kappa_3 = 1$. Furthermore, the robot has 10% a priori channel samples (200 samples) for channel assessment.

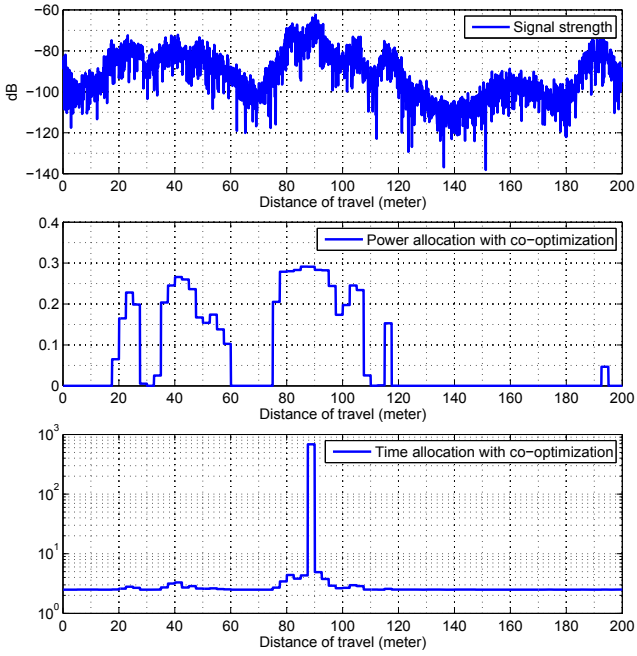

Fig. 2. The top figure shows the signal strength along the trajectory, and the middle and bottom figures show the optimum allocated power and time of our proposed co-optimization framework respectively.

Fig. 2 and 3 show the simulation results of our co-optimization framework. We compare the results with the case of no planning, i.e. uniform transmit power and time allocation. As can be seen from Fig. 2 (middle and bottom), the robot allocates more resources to the places that have a better communication quality. Fig. 3 shows the total number of transmitted bits per Hz as the robot travels along the trajectory. It can be seen that the robot performs significantly better by applying the co-optimization framework, as compared to the case of no planning. In this case, the average CNR over the trajectory is large enough such that the benefit of the additional water-filling is negligible.[1]

Fig. 4 shows the result when the average CNR over the whole trajectory is considerably low (i.e. 10 dB lower than the previous case). Our co-optimization frame also performs considerably better than the case of no planning. Moreover, in this case, the additional water-filling approach of Eq. 10 can further provide a non-negligible performance improvement.

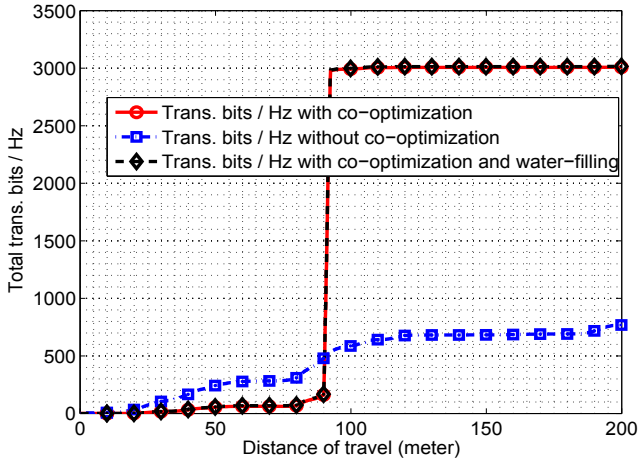

Fig. 3. Performance of our co-optimization framework. The plot shows the total number of transmitted bits per Hz along the trajectory.

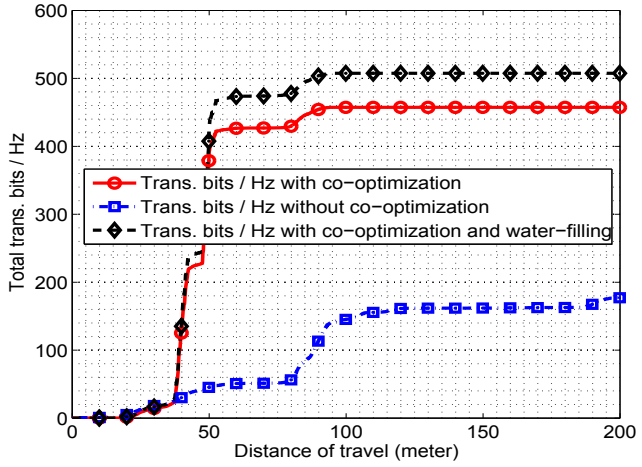

Fig. 4. Performance of our co-optimization framework, when the average CNR over the whole trajectory is considerably low. The plot shows the total number of transmitted bits per Hz along the trajectory.

[1]Note that if the total given time budget is small, then the optimum time allocation of Fig. 2 (bottom) becomes more uniform.

VI. Conclusion

In this paper, we considered a scenario where a robot needs to transmit as many bits of information as possible to a fixed station as it travels along a predefined trajectory. We considered the case where the robot operates under energy and time constraints and has to consider both its motion and communication costs. We proposed a co-optimization framework to allow the robot to adapt its velocity, motion energy and transmission rate/power along the trajectory, by using probabilistic online learning of wireless channels. Furthermore, the robot utilizes an additional water-filling approach to fine tune its resource allocation as it moves along its trajectory and measures the true value of the channel. Our mathematical framework and simulation results showed how our proposed framework results in a considerably more efficient use of the available resources.

References

[1] Jean-Claude Latombe. *Robot Motion Planning*. Kluwer Academic Publishers, 1991.

[2] C. Belta and V. Kumar. Abstraction and control for groups of robots. *IEEE Transactions on robotics*, 20(5):865–875, October 2004.

[3] C. E. Perkins and E. M. Royer. Ad-hoc on-demand distance vector routing. In *Proc. of the 2nd IEEE Workshop on Mobile Computing Systems and App.*, pages 90–100, New Orleans, Louisiana, Feb. 1999.

[4] R. Olfati-Saber. Flocking for multi-agent dynamic systems: Algorithms and theory. *IEEE Transactions on Automatic Control*, 51(3):401–420, March 2006.

[5] J. Laneman, D. Tse, and G. Wornell. Cooperative diversity in wireless networks: Efficient protocols and outage behavior. *IEEE Transaction on Information Theory*, 50(12):3062–3080, December 2004.

[6] A. Ghaffarkhah and Y. Mostofi. Channel learning and communication-aware motion planning in mobile networks. In *Proceeding of IEEE ACC*, pages 5413–5420, Baltimore, MD, July 2010.

[7] M. M. Zavlanos and G. J. Pappas. Potential fields for maintaining connectivity of mobile networks. *IEEE Trans. on Robotics*, 23(4):812–816, Aug. 2007.

[8] D. Tardioli, A. R. Mosteo, L. Riazuelo, J. L. Villarroel, and L. Montano. Enforcing network connectivity in robot team missions. *International Jounarl of Robotics Research*, 29(4):460–480, April 2010.

[9] M. Lindhé and K. H. Johanson. Using robot mobility to exploit multipath fading. *IEEE Wireless Comm.*, 16(1):30–37, Feburary 2009.

[10] N. Bezzo and R. Fierro. Tethering mobile routers. In *Proceedings of the IEEE ACC*, pages 6828–6833, Baltimore, MD, June 2010.

[11] C. C. Ooi and C. Schindelhauer. Minimal energy path planning for wireless robots. *Mobile Networks and App.*, 14(3):309–321, Jan. 2009.

[12] Y. Yan and Y. Mostofi. Robotic router formation in realistic communication environments - a bit error rate approach. *IEEE Transactions on Robotics*, 2010. conditionally accepted.

[13] Y. Mostofi, M. Malmirchegini, and A. Ghaffarkhah. Estimation of communication signal strength in robotic networks. In *Proceedings of the 50th IEEE ICRA*, pages 1946–1951, Anchorage, AK, May 2010.

[14] M. Malmirchegini and Y. Mostofi. On the spatial predictability of communication channels. *IEEE Trans. on Wireless Comm.*, preprint. available at http://www.ece.unm.edu/∼ymostofi/papers/TWC11.pdf.

[15] A. Goldsmith. *Wireless Communications*. Cambridge University Press, 2005.

[16] P. Wolm, X. Chen, J. G. Chase, W. Pettigrew, and C. E. Hann. Analysis of a pm dc motor model for application in feedback design for electric-powered mobility vehicles. *International Journal of Computer Applications in Technology*, 39(1):116–122, 2010.

[17] Y. Mei, Y.-H. Lu, Y. C. Hu, and C. S. G. Lee. Energy-efficient motion planning for mobile robots. In *Proceeding of IEEE ICRA*, pages 4344–4349, New Orleans, LA, April 2004.

[18] J. Nocedal S. J. Wright. *Numerical Optimization*. Springer, 2nd edition, 2006.

[19] A. Gonzalez-Ruiz, A. Ghaffarkhah, and Y. Mostofi. A comprehensive overview and characterization of wireless channels for networked robotic and control systems. *Journal of Robotics*, 2011. to appear.